

HSP20 peptide decreases human airway constriction downstream of β_2 adrenergic receptor

Alex Banathy¹, Joyce Cheung-Flynn¹, Kasia Goleniewska², Kelly L. Boyd³, Dawn C. Newcomb², R. Stokes Peebles Jr^{2,4}, and Padmini Komalavilas^{4,1*}.

Online data supplement

Materials and Methods: Pre-cast acryl amide gels, Sodium dodecyl sulfate (SDS), Tris-glycine-SDS buffer (TGS), Tris-glycine (TG), BioLyte, and prestained Precision Blue Protein Standards were purchased from Bio-Rad (Hercules, CA). Urea and 3-[(3-Cholamidopropyl) dimethylammonio]-1-propanesulfonate hydrate (CHAPS) were from Research Organics Inc. (Cleveland, OH). F/G Actin assay kit was from Cytoskeleton Inc., (Denver, CO).

Human Lung procurement and Physiological measurement of smooth muscle functional viability

Non-transplantable human lungs were collected after obtaining approval of the Institutional Review Boards of the VA Medical Center, Vanderbilt University Medical Center and the Tennessee Donor Services (TDS) (Nashville, TN). Lungs were immediately dissected and the bronchial airway (second generation) were isolated and stored in cold transplant harvest buffer [100 mM potassium lactobionate, 25 mM KH_2PO_4 , 5 mM MgSO_4 , 30 mM raffinose, 5 mM adenosine, 3 mM glutathione, 1 mM allopurinol, 50g/L hydroxyethyl starch, pH 7.4]. Bronchial rings were also dissected from porcine lungs collected from euthanized healthy pigs from the Surgical Suite at Vanderbilt University Medical Center or from the abattoir

(Triune, TN). Bronchial rings (5-7 mm diameter) were dissected free of connected tissue and epithelium and were equilibrated in an organ bath, in bicarbonate buffer (120 mM NaCl, 4.7 mM KCl, 1.0 mM MgSO₄, 1.0 mM NaH₂PO₄, 10 mM glucose, 1.5 mM CaCl₂, and 25 mM Na₂HCO₃, pH 7.4), with 95% O₂ and 5% CO₂ for 3 hrs. Each ring was progressively stretched to its optimal resting tension (approximately 1 gm) that would produce a maximal response to carbachol as determined previously, then maintained at the resting tension and equilibrated for a minimum of 3 hours E (1). Rings were rinsed 3 times every 15 min for the first hour, manually stretched to ~3gm and then equilibrated for additional two hrs set at a basal tension of 1gm. Force measurements were obtained using a Radnoti Glass Technology (Monrovia, CA) force transducer (159901A) interfaced with a Powerlab data acquisition system and Chart software (AD Instruments, Colorado Springs, CO). The rings were primed by contracting with CCH (10⁻⁶M) twice and rinsed and then contracted with 110mM KCl (with equimolar replacement of NaCl in bicarbonate buffer). Dose response for CCH (0.01-1 μM) and ISO (0.001-1 μM) were then determined and a dose of CCH that gives about 50-60% of KCl contraction was chosen (0.15-0.25 μM). HASM or PASM rings were contracted with CCH (0.15-0.25 μM) and then relaxed with ISO, (0.001-1 μM) or P20/or scrambled peptide (0.5-2 mM). To determine the inhibition of constriction, HASM or PASM rings were pretreated with ISO (0.5 μM) for 5 min or P20 peptide (1-2 mM) for 20 min and then challenged with CCH (0.15-0.25 μM) and the force generated was measured. Some rings were treated with a β₂-adrenergic receptor antagonist ICI 118551(0.2 μM) for 1 hr before adding the relaxants. Contraction and relaxation of ASM rings from mouse trachea were determined as

described for the HASM except that basal tension was adjusted to 0.3 gm on a 2 gm scale using 0.05 tungsten ring supports instead of 0.15 tungsten wire supports for HASM and PASM. Mice aortae were equilibrated in the muscle bath as described above and was manually stretched and primed with repeated KCl contraction. Dose response for phenylephrine (PE, 0.01-1 μ M) and sodium nitroprusside (SNP, 0.001-1 μ M) were then determined and a dose of PE that gave about 50-60% of KCl contraction was chosen (0.05-0.1 μ M). Mouse aortic rings were contracted with PE (0.05-0.1 μ M) and then relaxed with SNP (0.001-1 μ M). To determine the role of phosphorylation of proteins, physiologic experiments were conducted as described above and the tissues were snap frozen under tension using forceps precooled in liquid nitrogen and then pulverized. The pulverized tissues were stored at -80°C for later analysis using SDS polyacrylamide gel electrophoresis (PAGE) or isoelectric focusing and western blotting. Contractile response was defined as stress ($[10^5 \text{ Newtons (N)/m}^2] = \text{force (g)} \times 0.0987 / \text{area}$, where area is equal to the wet weight $[(\text{mg}) / \text{length (mm at maximal length)}]$ divided by 1.055), which was calculated using the force (g) generated by the tissue. Percent relaxation was calculated as the change in stress compared to the maximal tension induced by CCH as described previously E(1).

Determination of HSP20 phosphorylation

Phosphorylation of HSP20 in response to ISO was examined by isoelectric focusing, which separates the phospho- and non-phospho forms of HSP20 and detected by western blotting. Proteins from frozen muscle rings were extracted in UDC buffer (8 M urea, 10 mM dithiothreitol (DTT), 4% CHAPS containing protease inhibitor, Phosphatase I and II inhibitor cocktail (Sigma, St. Louis, MO). The

mixtures were vortexed at room temperature for 4 hr, and then centrifuged at 14,000 rpm for 15 min at 4°C. Soluble protein concentrations were determined using the Bradford assay (Pierce Chemical, Rockford, IL). 30 µg of extracted proteins from the treated HASM and PASM samples were separated on one-dimensional isoelectric focusing gel (8.3X7.3 cm) with 5% ampholines (4 parts pl 4-7 and 1 part pl 3-10, GE Healthcare Bio-Sciences) using 20 mM sodium hydroxide as a cathode buffer and 10 mM phosphoric acid as an anode buffer. Proteins were focused at 100 V for 1 hr, 250 V for 1 hr and 500 V for 30 min and transferred to nitrocellulose membrane (Li-COR Biosciences, Lincoln, NE) at 25 V in 0.7% acetic acid with the direction of the gel sandwich reversed (acetic acid give proteins a positive charge) for 1 hr at room temperature. The membranes were blocked prior to incubation overnight at 4°C with anti-HSP20 (1:5,000 dilution, Advanced Immunochemical Inc., Long Beach, CA) antibody. Membranes were washed three times with TBS containing Tween 20 (0.1%) (TBST), and incubated with appropriate infrared-labeled secondary antibodies (Li-Cor, Lincoln, NE) for 1h at room temperature. The membranes were subsequently washed with TBST, and protein-antibody complexes were visualized and quantified using the Odyssey direct infrared fluorescence imaging system (Li-Cor). Phosphorylation was calculated as a ratio of the phosphorylated protein to total (phospho+non-phospho) protein and was then normalized to the unstimulated control with the control value set as 1.0.

Cytoskeletal dynamics

The amount of F-actin versus G-actin was measured using the G-actin/F-actin *In Vivo* Assay kit (Cytoskeleton, Denver, CO), per manufacturer's protocol as

described previously E (2) . Briefly, treated ASM samples were homogenized in 1 ml of lysis buffer (50 mM PIPES pH 6.9, 50 mM NaCl, 5 mM MgCl₂ 5 mM EGTA, 5% (v/v) Glycerol, 0.1 % Nonidet P40, 0.1% Triton X-100, 0.1% Tween 20, 0.1% 2-mercapto-ethanol, 0.001% Antifoam C, 4 μM Tosyl arginine methyl ester, 15 μM Leupeptin, 10 μM Pepstatin A, 10 mM Benzamidine, 1 mM ATP warmed to 37°C) for 1 min with a mortar and pestle that fit into the 1.5 ml microfuge tube. The lysate was centrifuged at 2000 rpm for 5 min at 37°C to pellet unbroken cells. The supernatants were centrifuged at 100,000 x g for 1 hr at 37°C. Supernatants (contain the G-actin) were transferred to pre-cooled tubes and placed on ice. The pellets (contain F-actin) were resuspended in 1 ml of ice-cold 10 μM cytochalasin D in deionized water, and F- actin was depolymerized by incubating for 1 hr on ice with mixing every 15 min. Equal volume of supernatants and pellets along with actin standards (10-50 ng) were separated on 12% SDS-polyacrylamide gels and transferred to nitrocellulose membrane in 1 X TG buffer at 100 volts for 1 hr. The membrane was probed with anti-actin antibody and the amount of actin in each fraction was quantified comparing to actin standards loaded on the same gel.

Measurement of Stress fiber disruption and migration in human ASM cells

Primary HASM cells (Lonza Group Ltd. (Basel, Germany) were grown in growth medium (Lonza) containing 5% fetal bovine serum, insulin, human epidermal growth factor, human fibroblast growth factor B and gentamicin and were maintained in a 37°C and 5% CO₂ incubator. Cells were plated onto 18 mm cover glasses in 60-mm dishes (65–75% confluent), and serum starved for 24 hrs and were either left untreated or treated with CCH (0.15 μM), 200 μM P20 peptides, or 200 μM P20

peptides followed by CCH (0.15 μ M). Cells were washed three times in PBS (140mM NaCl, 2.7 mM KCl, 4.3mM Na₂HPO₄·7H₂O, 1.4mM KH₂PO₄, pH7.4) and fixed for 30 min in 4% (w/v) formaldehyde in PBS, washed in PBS, permeabilized in 0.1% (v/v) Triton X-100/PBS for 15 min at room temperature with gentle rocking, washed in PBS and blocked with 1% BSA in PBS for 15 min. Cells were processed for indirect immunofluorescence microscopy by adding Alexa568-conjugated phalloidin (1:1000 in PBS, Invitrogen) and DAPI (1:1000) and letting cells gently rock in the dark at RT for 1 h. Antibody concentration used was according to the manufacturer's instructions and was standardized for our experimental conditions. Following three washes with PBS, stained coverslips were inverted onto glass cover slides with ProLong gold antifade mounting medium (Invitrogen). Slides were dried for 24 h prior to sealing and imaging. The labelled cells were viewed using a Zeiss Axiovert 200M epifluorescence microscope (Carl Zeiss, Thornwood, N.Y., USA) equipped with a Xcite light source, and Alexa 568-conjugated phalloidin fluorescence images were obtained using filter sets for exciting Alexa 568 (ex 572/23 nm) and an Axiocam HR digital camera. Images were acquired and processed using Axiovision 4.5 and Photoshop software packages, respectively. Gain settings and exposure times were kept constant for all images taken. The intensity of the fluorescence was quantitated using Adobe Design Standard CS5 software from the ratio of the fluorescence intensity of the stress fibers over the total stained cell area. A fluorescence value above the background was set as the threshold for positive F-actin staining. The number of stress fibers per cell was calculated using Matlab as described earlier E (3). Briefly, the images were

uploaded into Matlab where custom software was used to map intensity of phalloidin fluorescence across a cell. By isolating the red channel intensity from the images acquired in Axiovision 4.5, a profile of intensity as a line function was created where peaks correlated to stress fibers stained with phalloidin. In the software a line function was created to draw, and then the selected 2D plot of distance across the cell vs intensity was mapped. The channel shown in the line intensity plot was the red fluorescence stain that binds to F-actin. Peak detection was conducted by finding peaks that were greater than 190 A.U. of fluorescence (set as a threshold for positive F-actin fiber staining since the background fluorescence outside of the stained cells was not greater than this value) within the cell which corresponded to the number of stress fibers.

To determine the migration using scratch assay, HASM cells were plated in a 6-well plate in 2 mL of complete medium and allowed to grow until 60% confluency. The cells were washed with HEPES-BSS and serum starved (0.1% FBS) for 24 hr at 37°C/5% CO₂. A sterile pipet tip was used to scrape a straight line down the well and cells were then either left untreated or pre-treated with 200 µM P20 peptide (20 min) and then incubated with 10 ng/mL platelet derived growth factor (PDGF) for 24 hrs. Three pictures were taken per well at 0, and 24 hrs on a Zeiss Axiovert 200M epifluorescence microscope at a magnification of 10 x and the number of cells that invaded the scratch was determined.

Migration assay was also performed using the ibidi Culture-Insert as per the manufacturer (ibidi, Munich, Germany). The culture-inserts were placed in the individual wells of a six well plate. 70 µl of the HASM cell suspension (5×10^5 cells)

was applied into each well of the insert. After the cells were attached the culture-inserts were removed generating a well-defined cell free gap (500 μm). Cells were then either left untreated, treated with 10 ng/mL PDGF or pre-treated with 200 μM P20 peptide (20 min) followed by 10 ng/mL PDGF for 24 hrs and cell migration into the gap was observed. Images were taken (four pictures per well) at 0, and 24 hrs on a Zeiss Axiovert 200 M epifluorescence microscope at a magnification of 10x and the number of cells in the gap was determined.

Mouse model of OVA-induced airway inflammation

Pathogen free 8-10 week old female BALB/c mice were obtained from Charles River Laboratories. Mice were categorized into 3 groups: mock/PBS, OVA/PBS, OVA/P20 peptide with 8 mice per group. The protocol for the OVA model of ovalbumin sensitization/challenge and P20 peptide treatment is shown in figure 3A and has been previously described E (4, 5). Briefly, mice were sensitized to ovalbumin with an intraperitoneal injection of 10 mg ovalbumin (chicken ovalbumin, grade V, Sigma Chemical Co.) conjugated with 20 mg of aluminium hydroxide $[\text{Al}(\text{OH})_3]$ on Day 0. On days 14 through 17, mice in the OVA groups were exposed to aerosols of 1% ovalbumin using a jet nebulizer for 40 min each day. PBS or P20 peptide (1.5 $\mu\text{g}/\text{gm}$ body weight) was administered intranasally 30 min before each antigen challenge.

Determination of AHR in response to methacholine

To measure the effect of the P20 peptide on OVA-induced AHR, mice with OVA-induced airway inflammation were administered the P20 peptide 30 min prior to OVA challenge each day (days 14-17) and 30 min prior to being anesthetized with

pentobarbital sodium (85 mg/Kg) for invasive lung resistance measurements on day 18. To measure lung resistance, a tracheostomy tube was inserted into the trachea of the mouse and the internal jugular vein was cannulated for intravenous administration of methacholine. Mice were then placed in an invasive Buxco plethysmography chamber and mechanically ventilated (0.2 ml tidal volume at 150 breaths/min using a Hugo Sachs Elektronik Mini-Vent type 845). Baseline resistance was established by ensuring mice were appropriately anesthetized, breathing with the assistance of the ventilator, and by performing two positive-end expiratory pressure (PEEP) maneuvers. PEEP was set to 2 cm H₂O for the experiment. Lung resistance, compliance, and elastance was measured following administration of intravenous acetyl- β -methacholine (0-1850 μ g/Kg body weight) by determining the changes in pressures in the lung, measured via a pressure-transducer connected to the trachea cannula, and changes in flow, measured by a flow transducer fixed to the whole body box in which the mouse is temporarily housed. Resistance, compliance, and elastance measurements were acquired for a 10 second window following the addition of each methacholine dose. Methacholine doses were administered intravenously in increasing concentrations, and after each dose mice were allowed to recover to baseline resistance for 60-90 seconds E (4, 5).

Ex vivo responsiveness of isolated tracheal segments from OVA mice:

After the methacholine challenge, tracheas were isolated from the mice and the contractile function was measured in the muscle bath as described for HASM. Mouse ASM rings were contracted with 0.15 μ M CCH and then relaxed with ISO, (0.001 -1 μ M) or P20 peptide (2 mM) and the force generated was measured.

Differential cell counts in the bronchoalveolar lavage (BAL) fluid

Following lung resistance measurements, the animals were given a lethal injection of pentobarbital and BAL was performed by injection of 0.6 ml saline through a tracheal cannula into the lung as described E(6). The fluid was centrifuged and the cells were resuspended in cold PBS. Cytologic examination was performed on cytospin preparations (Shandon Southern Instruments, Sewickly, PA). Cytospin slides were fixed and stained using Diff Quick (American Scientific Products, McGaw park, IL). Differential counts were based on counts of 200 cells using standard morphologic criteria to classify the cells as either eosinophils, lymphocytes, or other mononuclear leukocytes (alveolar macrophages and monocytes).

Cytokine and Chemokine Analysis

Whole lung homogenates were analyzed for IL-5, IL-13, CCL11 (eotaxin 1), and CCL24 (eotaxin 2) protein expression by quantikine ELISA per manufacturer's directions (R and D systems).

Supplemental References

- E1. Komalavilas P, Penn RB, Flynn CR, Thresher J, Lopes LB, Furnish EJ, Guo M, Pallero MA, Murphy-Ullrich JE, Brophy CM. The small heat shock-related protein, hsp20, is a camp-dependent protein kinase substrate that is involved in airway smooth muscle relaxation. *Am J Physiol Lung Cell Mol Physiol* 2008;294(1):L69-78.
- E2. Hocking KM, Baudenbacher FJ, Putumbaka G, Venkatraman S, Cheung-Flynn J, Brophy CM, Komalavilas P. Role of cyclic nucleotide-dependent actin cytoskeletal dynamics: $[Ca^{2+}]_i$ and force suppression in forskolin-pretreated porcine coronary arteries. *PLoS One* 2013;8(4):e60986.
- E3. Evans BC, Hocking KM, Kilchrist KV, Wise ES, Brophy CM, Duvall CL. Endosomolytic nano-polyplex platform technology for cytosolic peptide delivery to inhibit pathological vasoconstriction. *ACS nano* 2015;9(6):5893-5907.
- E4. Peebles RS, Jr., Sheller JR, Johnson JE, Mitchell DB, Graham BS. Respiratory syncytial virus infection prolongs methacholine-induced airway hyperresponsiveness in ovalbumin-sensitized mice. *J Med Virol* 1999;57(2):186-192.
- E5. Peebles RS, Jr., Sheller JR, Collins RD, Jarzecka AK, Mitchell DB, Parker RA, Graham BS. Respiratory syncytial virus infection does not increase allergen-induced type 2 cytokine production, yet increases airway hyperresponsiveness in mice. *J Med Virol* 2001;63(2):178-188.
- E6. Newcomb DC, Boswell MG, Huckabee MM, Goleniewska K, Dulek DE, Reiss S, Lukacs NW, Kolls JK, Peebles RS, Jr. IL-13 regulates Th17 secretion of IL-17A in an IL-10-dependent manner. *Journal of immunology* 2012;188(3):1027-1035.

Figure Legends

Figure E1. Inhibition of F-actin stress fiber formation in HASM cells. A) F-actin stress fiber quantitation. Representative epifluorescence micrographs at 20X magnification of HASM cells showing stress fiber formation when the cells were untreated (untreated), treated with 0.15 μ M CCH (CCH), treated with P20 peptide (200 μ M for 20 min, P20), with P20 peptide (200 μ M) for 20 min prior to CCH (0.15 μ M, P20+CCH) with the respective intensity profile below. The number of stress fibers per cell was calculated from three intensity profiles taken from the axis transverse to the cellular polarity from 6-7 cells per treatment group and derived from the line shown in the image. B) Cumulative data showing the number of stress fibers per cell. P20 peptide significantly decreased CCH-induced stress fiber formation, *** untreated vs CCH, $p < 0.0001$, *** CCH vs P20, $p < 0.0001$; * CCH vs P20+CCH, $p < 0.05$, p values calculated using 1 way ANOVA with Tukey's Multiple Comparison Test.

Figure E2. P20 peptide significantly reduced PDGF-induced migration of HASM cells. HASM cells were treated with P20 peptide (200 μ M, 20 min), PDGF-BB (10 ng/mL), or pretreated with P20 (200 μ M, 20 min) prior to PDGF-BB (10 ng/mL). Cells were allowed to grow for 24 hrs and pictures and migratory cell counts were made at 0 and 24 hrs. PDGF-BB significantly increased the number of migratory cells at 24 hrs (compared to control, * $p = 0.01$) and P20 peptide treatment blocked the increase in migration induced

by PDGF (* p=0.018), ns= nonsignificant, control vs P20, n=6, p values calculated using 1 way ANOVA with Tukey's Multiple Comparison Test.

Figure E3. Toxicity study of the P20 peptide: Mice were treated with PBS, P20 peptide 2 µg/gm or 5 µg/gm body weight for 5 days intranasally in 100 µl PBS. Representative Hematoxylin and eosin stained sections (200x magnification) of liver, kidney, lung and heart demonstrating no pathology when treated with P20, n=5.

Figure E4. Resistance, Compliance and Elastance changes with P20 peptide in OVA mice. Mice were mock sensitized and treated with PBS (mock/PBS) or sensitized and challenged with ovalbumin and treated with either PBS (OVA/PBS) or 1.5 µg/gm body weight P20 peptide in 100 µl PBS intranasally for 5 days (OVA/P20) and challenged with methacholine as described in the methods section and lung resistance (A), compliance (B) and elastance (C) were measured. ** Significant OVA/PBS vs OVA/P20 and mock/PBS vs OVA/PBS, n=4-9, p<0.001, ns, nonsignificant, p values were calculated using 2 way ANOVA with Bonferroni posttests.

Figure E5. *EX Vivo* contraction and relaxation of trachea isolated from OVA sensitized mice. After methacholine challenge the tracheas were harvested from the mock sensitized mice (mock/PBS), OVA sensitized (OVA/PBS) and OVA sensitized and treated with P20 peptide (1.5 µg/gm body weight, OVA/P20) mice and hung in a muscle bath and equilibrated as described in the methods section. Tracheal rings were contracted with CCH (0.2 µM) and relaxed with various doses of ISO (0.001 to 1 µM) and force generated was measured. A representative tracing is shown n=4-6.

Figure E6. P20 peptide does not reduce the OVA-induced increase in IL-5 and IL-13 protein expression in lung homogenates. Mice were mock sensitized and treated with PBS (mock/PBS) or sensitized and challenged with ovalbumin and treated with either PBS (OVA/PBS) or 1.5 $\mu\text{g}/\text{gm}$ body weight P20 peptide in 100 μl PBS intranasally for 5 days (OVA/P20). IL-5 (panel A) and IL-13 (panel B) protein expression was measured in the lung homogenates. Panel A,B, * $p < 0.05$, *** $p < 0.001$, ns= non significant, $n = 4-6$ mice per group, one-way ANOVA with Tukey's multiple comparison test. Panel C,D. P20 peptide does not reduce the OVA-induced increase in CCL11 (eotaxin 1) and CCL24 (eotaxin 2) in whole lung homogenates. Mice were mock sensitized and treated with PBS (mock/PBS) or sensitized and challenged with ovalbumin and treated with either PBS (OVA/PBS) or 1.5 $\mu\text{g}/\text{gm}$ body weight P20 peptide in 100 μl PBS intranasally for 5 days (OVA/P20). CCL11 and CCL24 protein expression was measured in the lung homogenates. *** $p < 0.001$, ns= non significant, $n = 4-6$ mice per group, one-way ANOVA with Tukey's multiple comparison test.

Figure E7. P20 peptide treatment does not affect contractility of aortae in mice *ex vivo*. Mice were treated with PBS or P20 peptide (2 and 5 $\mu\text{g}/\text{gm}$ body weight) in PBS intranasally for 5 days and the aortae were harvested and hung in a muscle bath and equilibrated as described for HASM in the methods section. Aortic rings were contracted with phenylephrine (0.1 μM) and relaxed with SNP (0.01 μM) and force generated was measured and converted to stress. A) contractile response to phenylephrine, ns=not significant between PBS and P20 peptide 2 or 5 $\mu\text{g}/\text{gm}$,

p=0.518, n=4, B) percent relaxation to SNP. ns=not significant between mock and P20 peptide 2 or 5 $\mu\text{g}/\text{gm}$, p=0.522, n=4, p values calculated using 1 way ANOVA with Tukey's Multiple Comparison Test.

Supplemental Tables

Table E1. Complete Blood Count Results with P20 peptide

| | PBS | P20 2 µg/gm | P20 5 µg/gm |
|-------------|--------------|--------------|--------------|
| WBC (K/µl) | 5.712±1.365 | 5.996±0.560 | 6.690±0.524 |
| NE# (K/µl) | 1.534±0.485 | 1.554±0.161 | 2.212±0.292 |
| LY# (K/µl) | 3.582±0.853 | 3.740±0.358 | 3.887±0.239 |
| MO# (K/µl) | 0.406±0.038 | 0.582±0.061 | 0.562±0.039 |
| EO#(K/µl) | 0.142±0.052 | 0.082±0.035 | 0.025±0.015 |
| BA# (K/µl) | 0.050±0.015 | 0.034±0.011 | 0.012±0.006 |
| HCT (%) | 57.260±3.571 | 57.180±3.008 | 52.075±0.502 |
| RBC (M/µl) | 10.314±1.745 | 10.188±0.538 | 9.360±0.127 |
| HB (g/dl) | 15.460±1.138 | 15.440±0.722 | 14.075±0.216 |
| MCV (fL) | 55.460±0.524 | 56.160±0.261 | 55.650±0.350 |
| MCH (pg) | 14.960±0.385 | 15.160±0.146 | 15.025±0.103 |
| MCHC (g/dL) | 26.920±0.491 | 27.040±0.348 | 27.025±0.165 |

n=5 per group. No significant difference between groups.

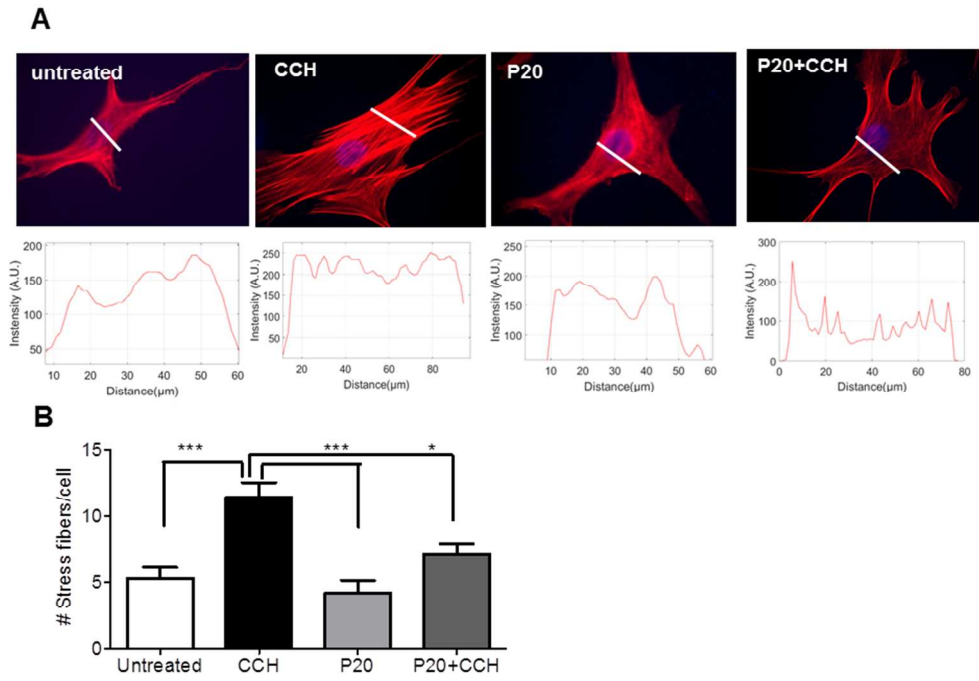


Figure E1
254x190mm (96 x 96 DPI)

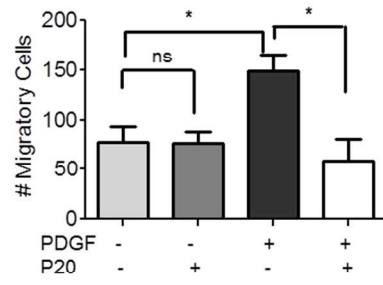


Figure E2
254x190mm (96 x 96 DPI)

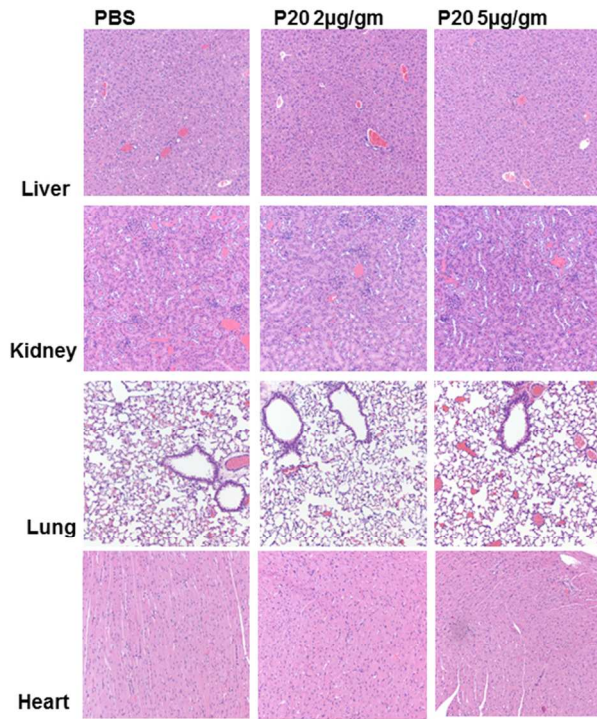


Figure E3
254x190mm (96 x 96 DPI)

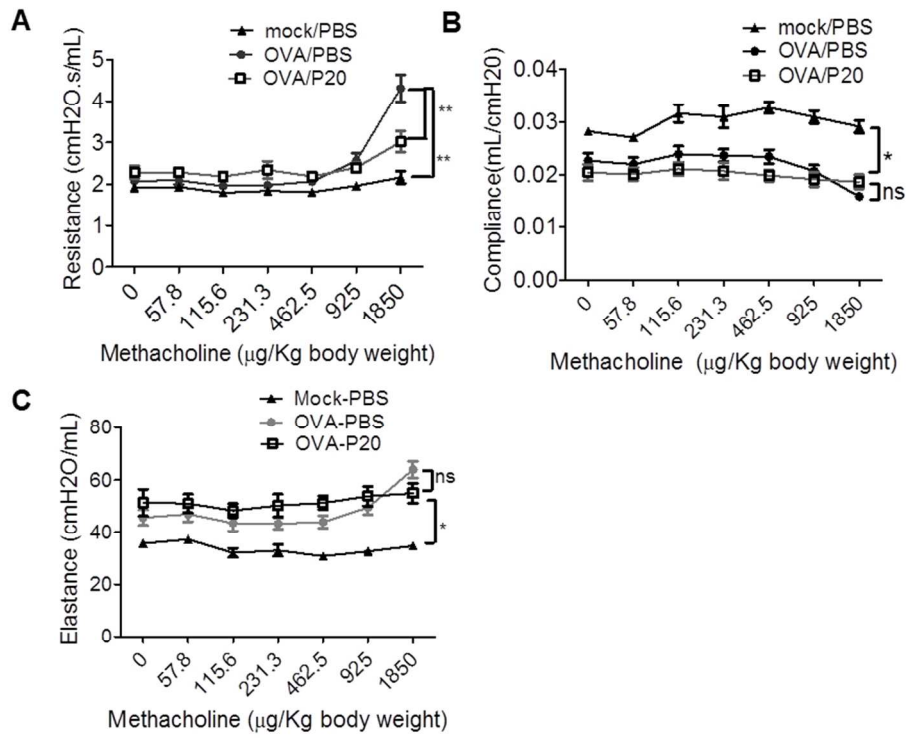


Figure E4
254x190mm (96 x 96 DPI)

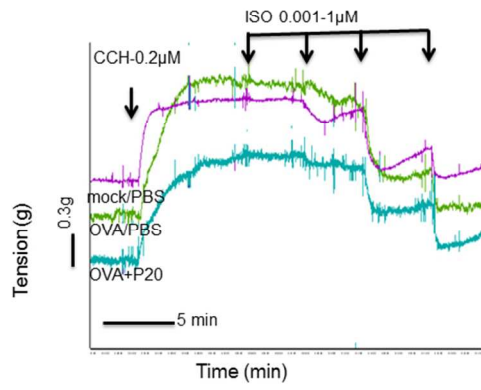


Figure E5
254x190mm (96 x 96 DPI)

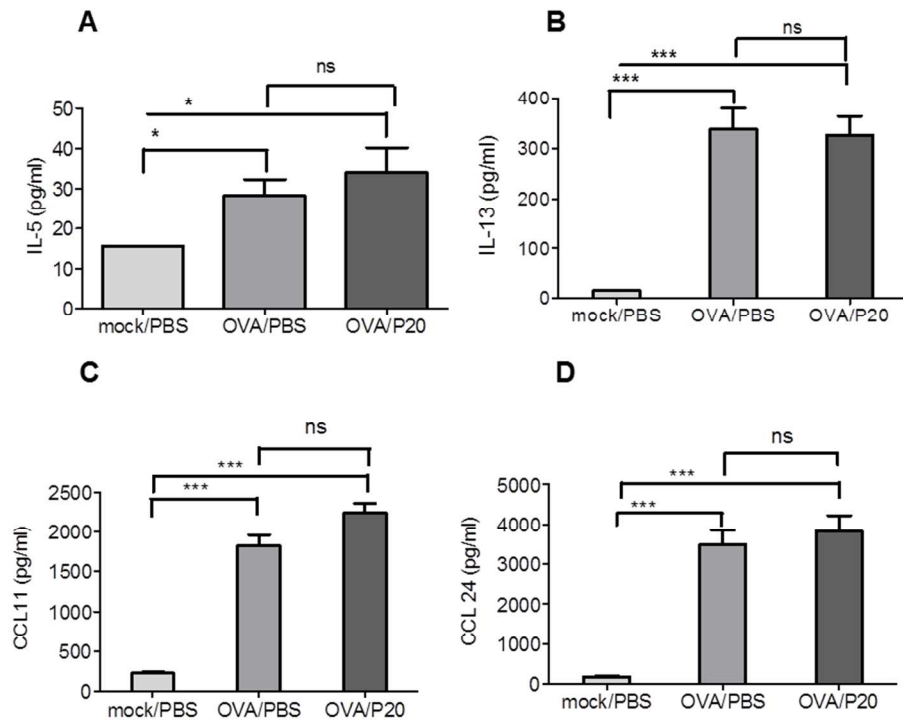


Figure E6
254x190mm (96 x 96 DPI)

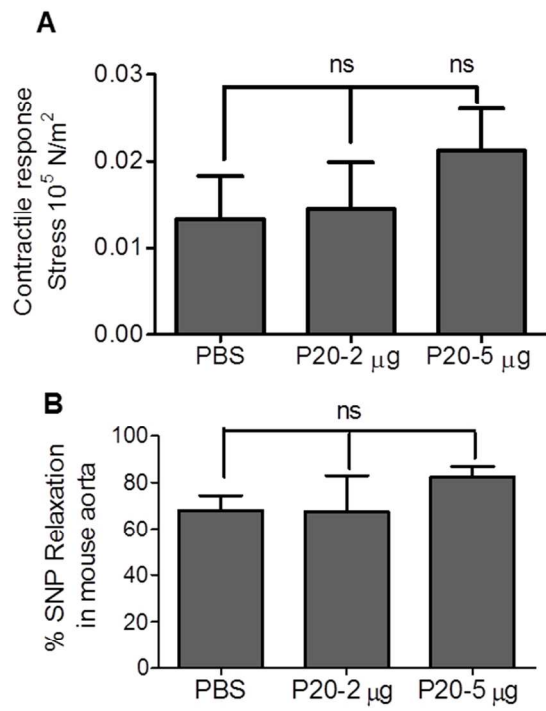


Figure E7
254x190mm (96 x 96 DPI)